

Review

# Strategies for Enhancing the Low Wind Speed Performance of H-Darrieus Wind Turbine—Part 1

Palanisamy Mohan Kumar <sup>1,\*</sup>, Krishnamoorthi Sivalingam <sup>2</sup>, Teik-Cheng Lim <sup>2</sup>,  
Seeram Ramakrishna <sup>1</sup> and He Wei <sup>3</sup>

<sup>1</sup> Centre for Nanofibers and Nanotechnology, Department of Mechanical Engineering, National University of Singapore, Engineering Drive 3, Singapore 117587, Singapore

<sup>2</sup> School of Science and Technology, Singapore University of Social Sciences, 463 Clementi Rd, Singapore 59949, Singapore

<sup>3</sup> Singapore Institute of Manufacturing Technology, Surface Technology group, A\*STAR, Fusionopolis way 2, Innovis, Singapore 138634, Singapore

\* Correspondence: mohan@nus.edu.sg or to\_mohankumar@yahoo.com

Received: 4 July 2019; Accepted: 29 July 2019; Published: 2 August 2019



**Abstract:** Small wind turbines are key devices for micro generation in particular, with a notable contribution to the global wind energy sector. Darrieus turbines, despite being highly efficient among various types of vertical axis turbines, received much less attention due to their starting characteristics and poor performance in low wind speeds. Radically different concepts are proposed as a potential solution to enhance the performance of Darrieus turbine in the weak wind flows, all along the course of Darrieus turbine development. This paper presents a comprehensive review of proposed concepts with the focus set on the low wind speed performance and critically assessing their applicability based on economics, reliability, complexity, and commercialization aspects. The study is first of its kind to consolidate and compare various approaches studied on the Darrieus turbine with the objective of increasing performance at low wind. Most of the evaluated solutions demonstrate better performance only in the limited tip speed ratio, though they improve the low wind speed performance. Several recommendations have been developed based on the evaluated concepts, and we concluded that further critical research is required for a viable solution in making the Darrieus turbine a low speed device.

**Keywords:** VAWT; low wind speed; Darrieus; self-starting; power coefficient; drag; airfoil; Giromill; camber

## 1. Introduction

Energy is the vital ingredient for global growth and is undoubtedly the fundamental driver for the economic progress of a country. The demand for energy increases exponentially due to rapid population growth and the rise in per capita energy consumption. For sustainable economic growth, it is imperative for countries to generate sufficient energy. With global warming and the unpredictable climate changes, the energy industry is being compelled to find alternative sources of clean energy, which is free from greenhouse gases. Utilization of renewable energy has seen a tremendous acceleration due to fossil fuel depletion, rising energy demand, and sustainability. Among various renewable energy sources, wind and solar energy are cost effective and implementable in required capacities. Wind energy is a major clean energy source that has acquired great momentum across the world in the past years. The global cumulative installed capacity of wind power rose from 24 GW in 2001 to 587 GW in 2017 [1]. The primary types of wind turbines are Horizontal Axis Wind Turbines (HAWTs) and Vertical Axis Wind Turbines (VAWTs). The HAWTs are more efficient than VAWTs and are

commercially exploited for large scale power production [2]. The VAWTs are preferred for small scale power generation due to their unique advantages such as Omni directionality [3], lower manufacturing cost, the benefit of a generator on the ground level, and low noise. As VAWTs are preferred for roof top installations, the skewed flow must be accounted for. Wind tunnel test on both HAWT and VAWT shows that VAWT perform better than HAWT in skewed flow, even up to 30°. Among VAWTs, the turbines are categorized as lift and drag based. The Savonius turbines are based on the drag difference between the rotating blades. Despite its lower efficiency and maximum power coefficient of 0.18 [4], these types of turbines are preferred for low wind conditions due to high dynamic moment as demonstrated in a recent study [5]. The lift based Darrieus turbines are preferred for moderate wind speeds with the power coefficient of 0.35~0.38 [6]. Since the small wind turbines are often installed in the locations of power demand [7] rather than optimum wind speed condition. As high wind sites are exploited to the fullest, these turbines find their locations that have an average wind speed of 4~6 m/s. Darrieus turbines are notoriously bad performers in these wind speeds due to their non-self-starting nature and very low torque due to the aerodynamics that are associated with the Darrieus rotor configuration.

The search for a feasible solution to enable a Darrieus turbine to generate optimal power at low wind speed continue for decades. Over these years, countless efforts have been made through experimental, computational and field tests to achieve significant progress in understanding self-starting physics of Darrieus turbine. These attempts substantially improved the starting behavior of these turbines, yet they are still not preferred for low wind speed sites due to their low annual energy output. Another limiting factor for these turbines is the lack of forms of aerodynamic power regulation such as furling or blade pitching as in the case of HAWT. The objective of the current literature search is to identify a feasible solution that will enable the Darrieus rotor to generate power rather than self-starting. The existing strategies are critically examined with the constraints on cost, ease of maintenance, reduced complexity, and high reliability. The concept behind each strategy is discussed in detail, with a sketch of the Darrieus turbine incorporating the same. Power coefficient of each strategy is compared with the conventional turbine to quantify the performance loss or gain. The chapter ends with a comparative Table 1 listing the strategies as well as their merits and demerits.

## 2. Airfoil Characteristics

The airfoil geometric features and their aerodynamic characteristics have a profound effect on turbine performance and starting characteristics. The airfoil characteristics evaluated in this text pertains to small fixed pitch straight bladed Darrieus turbine of power capacity less than 20 kW that may typically operate at the rated wind speed of 10~12 m/s. Though a high coefficient of lift/coefficient of drag ( $C_l/C_d$ ) ratio is preferred for any airfoil design, a maximum  $C_l/C_d$  over a wider range of angle of at tack (AoA) is the desired characteristics for vertical axis wind turbines. The chosen airfoil should be able to generate sufficient lift both in the positive angle of incidence during the upstream half and the negative angle of incidence in the downstream half. The airfoil exhibits the lowest drag for a narrow AoA termed as “drag bucket”, as suggested by Islam [8]. A wider drag bucket is a desirable property to maintain the performance over a larger AoA. Laneville [9] identified that stall angle at a low Reynolds number (Re) has a strong influence on the performance at low wind speed and when the turbines are self-starting. The Darrieus turbines are sensitive to change in Re, but the degree of sensitivity depends on the range of Re its is operating. The sensitivity of turbine power coefficient ( $C_p$ ) to Re, with sensitivity diminishing at the higher Reynolds numbers, especially for turbines of lower solidity. A stalled blade at low tip speed ratio (TSR) fails to incite the rotation there by delaying the acceleration of the rotor. Hence an airfoil that has wider stall angle at low Re is preferred. Deep stall behavior has a detrimental effect on the performance and should be postponed to higher AoA. Timmer [10] found that a linear correlation exists between the thickness of the airfoil and deep stall angle. Jasinski [11] studied the effect of surface roughness on the performance of airfoil in low Re and found that a high surface roughness at the leading edge will induce turbulent flow over an entire

airfoil. It was found that blade roughness affects negatively turbine performance. The performance found to be decreasing as the blade roughness increases and it is irrespective of turbine solidity. The blade roughness is much more significant at high blade  $Re$  compared to low  $Re$ . Hence a significant weighting factor on surface roughness should be accounted for while selecting an airfoil.

Most of the fixed pitch Darrieus turbines are installed in an urban environment, where noise is one of the deciding factors as suggested by Shepherd [12]. The noise in the straight bladed turbine is generated when the laminar separation bubble leaves the trailing edge by inducing vibrations. Kato [13] claimed that the pitching moment coefficient of the airfoil should be higher for increased power performance. His study shows that high power coefficient ( $C_p$ ) is achieved when the moment coefficient  $C_m = 0.05$  than  $C_m = 0$ . The  $C_m$  value is higher for the camber blades, whereas for the symmetric blades it oscillates around zero. Myriad airfoils were proposed for Darrieus turbine in the past decades with the objective of promoting self-starting and to reduce the manufacturing cost. Following are the prerequisites for selecting an airfoil.

- i. Operating wind speed range— $Re$  range.
- ii. Fixed pitch or pitch able blades.
- iii. Straight blades or helical blades.
- iv. Installation environment-urban or rural location.
- v. Self-start or assisted start such as motor start
- vi. Drive train arrangement—Resistive torque and efficiency.
- vii. The manufacturing method of blades-Aluminum extrusion or moulding.

The need for optimized airfoil dedicated for VAWT arises in the late 1970s when the wind energy emerged as a key renewable source after energy crisis and to improve the performance of Darrieus turbine at par with the HAWT. The following is the list of prospective airfoils developed so far, as illustrated in Figure 1.

### 2.1. WSU 0015

The airfoil was developed by Snyder [14] at Wichita State University (WSU) in an effort to postpone the stall angle and attain peak performance at lower TSR. The experimental comparison of WSU 0021 with National Advisory Committee for Aeronautics (NACA) 0012 reveals that the synthesized WSU 0021 achieved a peak power coefficient of 0.25 at TSR 4, whereas the NACA 0012 can achieve 0.2 at TSR 5.

### 2.2. NACA00XX

Symmetrical NACA profiles are preferred during early days of VAWT development due to readily available test data that are meant for aviation purpose. Initially, NACA0012 was employed in smaller capacity turbines. As the size of the turbine grows bigger, NACA 0018 [15] is preferred for the structural stiffness. Several NACA 00XX profiles are evaluated for higher AoA and  $Re$  range suitable for larger VAWTs.

### 2.3. SAND00XX/XX

Sandia National Laboratories optimized early NACA profiles for sharp stall and wider drag buckets at high AoA. The resulted airfoils are designated as SAND 0015/47, SAND 0018/50 and SAND 0021/50 [16]. The last two digits indicate the location of laminar flow on the chord. The new airfoils are less sensitive to surface roughness and can be seamlessly integrated with other airfoils for performance improvement. The 500 kW test turbine comprises of both NACA 0021 at the root for structural rigidity and SAND 0018/50 at the equatorial region of Troposkein blade for aerodynamic performance.

#### 2.4. TWT 11215-1

The TWT airfoil series is an outcome of Tokai University research on VAWT development. The airfoil TWT 11215-1 was developed by Kato [13] employing the single stream tube model rather than the Double multiple stream model [17] with the objective of gaining a large pitching moment and minimal drag coefficient about zero lift line. The airfoil has negative camber on the leading edge and positive camber on the trailing edge giving rise to S-shaped camber line. The experimental results show that an increase in  $C_p$  was noted with an increase in the pitching moment.

#### 2.5. NACA 6 Series

NACA 64 and 63 series airfoils were optimized by Migliore [18] at West Virginia University and compared with traditional NACA 00XX airfoils. The results show a higher  $C_p$  at higher TSR than traditional airfoils. Subsequent testing revealed that the performance increases with the airfoil thickness, a desirable property from the structural perspective. NACA 632015, corrected for flow curvature effects outputs 20% more annual energy than NACA 0015.

#### 2.6. ARC Series

The ARC series of airfoils are conceived by the National University of Athens. The series was devised as a potential solution for the flow curvature effect on Darrieus turbine performance. It was found that the airfoil behaves differently when it is subjected to curvilinear flow and rectilinear flow. To counter the effect of flow curvature, a virtual camber and virtual angle of incidence are introduced on the symmetric airfoil in relation to the turbine radius. The airfoil camber value should be tailored for the given turbine parameters as chord ( $c$ )/ radius of curvature ( $R$ ) changes. Zervos [19] designated the flow curvature corrected airfoil of NACA 0015 as ARC 0015. An added advantage of ARC airfoils is the ability to diminish the unsteady loading, thereby extending the fatigue life of blades.

#### 2.7. DU 06-W-200

The Du series of airfoils were developed by Claessens [20] at Delft University with the aim of improving both the aerodynamic and structural characteristics. The airfoil DU 06-W-200 was conceived in an effort to increase the thickness of the airfoil without compromising the maximum lift coefficient. The optimized airfoil is 20% thick and 0.8% camber. An extensive wind tunnel comparison with NACA 0018 shows that the DU 06-W-200 airfoil performs similar to NACA 0018 for negative AoA, while an increased lift coefficient is reported at positive AoA. The deep stall occurs with a reduced drop in lift coefficient at higher AoA. The laminar separation bubble of DU 06-W-200 does not extend up to the trailing edge, as occurs in the case of NACA 0018. The Double Multiple Stream Tube (DMST) validation shows an 8% increment in the power coefficient and 108% improvement with a higher surface roughness than NACA 0018.

#### 2.8. LS-0417

The LS series was developed by McGhee [21] at NASA for low-speed general purpose aviation. The symmetric airfoil with 17% thickness was compared with NACA 0012, 0015 and 0018. The results demonstrate that instantaneous power coefficient, normal and tangential force coefficients are smoothly distributed with smaller peaks. The LS-0417 was compared with GOE 420, NACA 4415 and NLF-0416 [8] for the  $Re$   $1 \times 10^5$  to  $3 \times 10^5$ . The LS-0417 performed better than all the investigated airfoils, which later become the basis for the evolution of prospective airfoils.

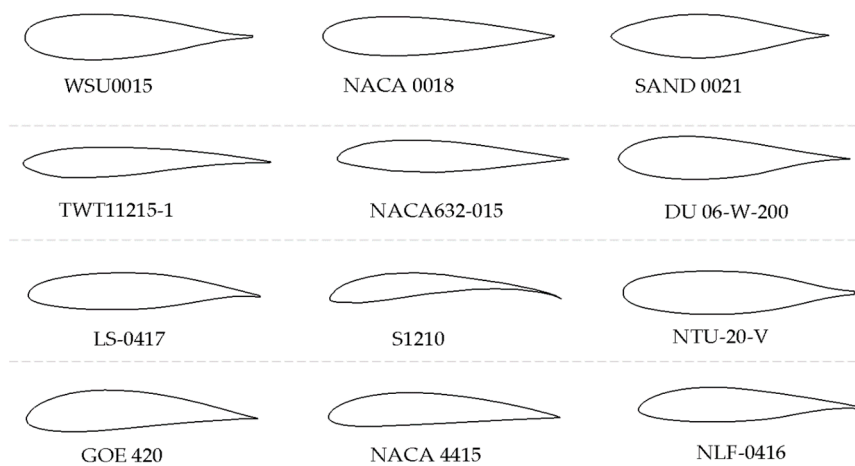


**Figure 1.** Prospective airfoils for VAWT.

### 2.9. S1210

S1210, high lift and low Re airfoil was considered by Islam [8] for VAWT from the self-starting perspective. Experimental verification indicates a high static torque coefficient ensures the self-starting capability. The maximum power coefficient of 0.32 was obtained for the rotor solidity of 0.1, after which a significant drop is noted. Singh [22] compared S1210 with NACA 0015 and found that the S1210 airfoil recorded a lower power coefficient due to reduced torque generation on the downstream half. The 7.2% camber is attributed to the poor downstream performance. Though S1210 may be appropriate for self-starting, 12% thickness will pose a challenge for achieving required structural stiffness.

### 2.10. NTU-20-V

The NTU-20-V airfoil was developed by Mohan [23] at Nanyang Technological University is a recent addition to the VAWTs airfoil list. The objective is to facilitate the manufacturing of inexpensive blades with extended fatigue life for smaller capacity turbines. Initial investigation with trapped vortex airfoil [24], followed with wind tunnel tests [25] shows promising results on low Re. Airfoils with modified trailing edges have also been studied for their ease of manufacturing [26]. With the constraints on thickness and lift coefficient genetic algorithm optimization has been carried out to generate the new airfoil profile that can accommodate standard shapes of carbon fiber material from NACA 0018 surface pressure distribution. The conceived airfoil is 20% thick at 37.5%c. A minimum thickness of 17% is extended over 40%c. The computational comparative study with NACA 0018 on VAWT for the Re range  $1.2 \times 10^5$  to  $2.7 \times 10^5$ , displayed almost the same power coefficient as parent airfoil, but at a higher TSR [27].

## 3. Camber and Symmetric Airfoils

The most popular choice of airfoils for Darrieus turbines are symmetrical NACA profiles such as NACA 0015, 0018, and 0021, as they are experimentally validated for the range of Re that a VAWT typically experiences while in operation. Though it seems logical and efficient to use symmetrical airfoils as the suction and pressure side are reversed during the upwind and downwind rotation, the cambered airfoils are preferred from the self-starting perspective, especially for the fixed pitch VAWT as evaluated by Rainbird [28]. The airfoils should generate sufficient lift at low Re of  $10^3$  to  $10^4$  to overcome the resistive and inertial torque of the turbine to self-start. The symmetrical airfoils exhibit poor performance in this range and thus failing to start at low wind speeds. In contrast, a cambered airfoil is able to generate moderate lift in this range of Re inducing rotation without significant abatement in power production at high winds. The cambered airfoils can be mounted in

concave out or concave in (concave side facing the rotor centre) configuration as shown in Figure 2a–c. Since the power output is proportional to the cube of wind speed, the upstream half of a rotor encounters high velocity compared to downstream half and hence it is wise to select a configuration that performs better in upstream half. To enhance the self-starting process with cambered airfoils, the concave out configuration extracts maximum power due to the positive angle of incidence in upstream half, whereas for the concave in configuration, the airfoil encounters a negative angle of incidence in the upstream half, leading to a reduced power output. Though cambered airfoils generate moderate drag on the downstream half due to negative incidence angle, the superior performance due to the positive angle of incidence in the upstream half will result in a higher overall performance at low Re. Wortmann FX63-137 airfoil of more than 5% camber was investigated by Islam [29] comparing with NACA 0012. The outcome is that the airfoil with strong laminar separation bubble phenomena before stall and lower post stall drag are desirable features for a fixed pitch VAWT. Zervos [19] compared NACA 63-015 with NACA 0012, 0015 and 0018 and found that cambered airfoil has a smooth distribution of normal and tangential forces over a wide range of azimuthal angle than instantaneous peak forces by symmetrical airfoils and thus extends the longevity of the blades and structures by reducing the fatigue stress. Kirke [30] suggested that the cost of manufacturing a symmetrical airfoil and cambered airfoil is almost the same with added minor tooling charges. Several studies in the past were carried out experimentally to ascertain the performance of cambered airfoil over symmetrical airfoil leading to the development of special airfoils for fixed pitch VAWT. NACA 0018 was theoretically compared with Gottingen series (GOE 460, GOE 676, GOE 738) of varying camber % and concluded that power output of the cambered airfoil was inversely proportional to camber % and experimentally compared with GOE 420. A highly cambered S1210 airfoil was compared with NACA 0015 by Healy [31], who concluded that the maximum  $C_p$  occurs at lower TSR for cambered airfoils than symmetrical airfoils as shown in Figure 3a. The cambered airfoils display larger stall angle due to the requirement of large adverse pressure gradient either on suction or pressure side of the airfoil. Another notable advantage of cambered airfoil is a higher pitching moment and less sensitivity to roughness compared to symmetrical airfoils. It can be noted that both the airfoils have a similar stall, which is favorable for vibration free operation. From the overall turbine performance, camber airfoil shows a superior performance to symmetric airfoils, especially for the turbines operating at low TSR. For the self-starting and low wind speed operation, cambered airfoils are a better choice and have been commercially implemented.

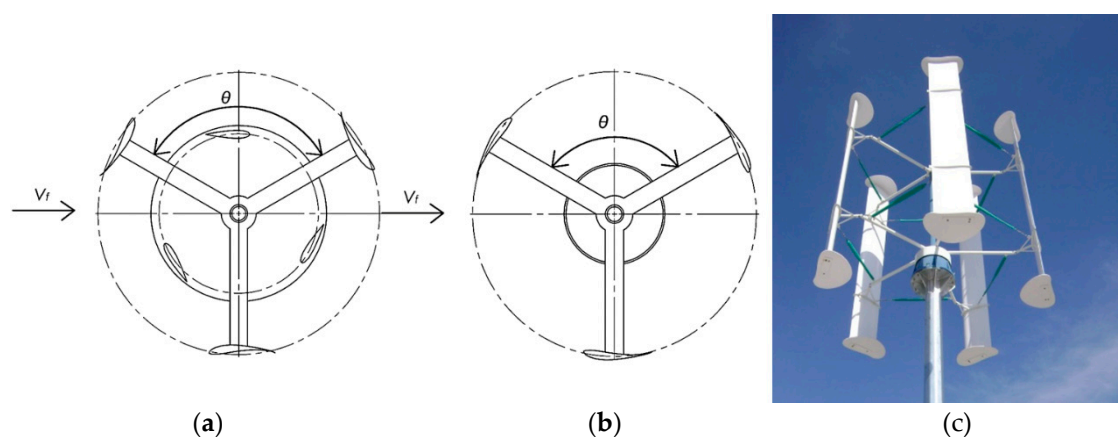


**Figure 2.** (a) Concave-In; (b) Concave-Out; (c) Turbine with cambered blades.

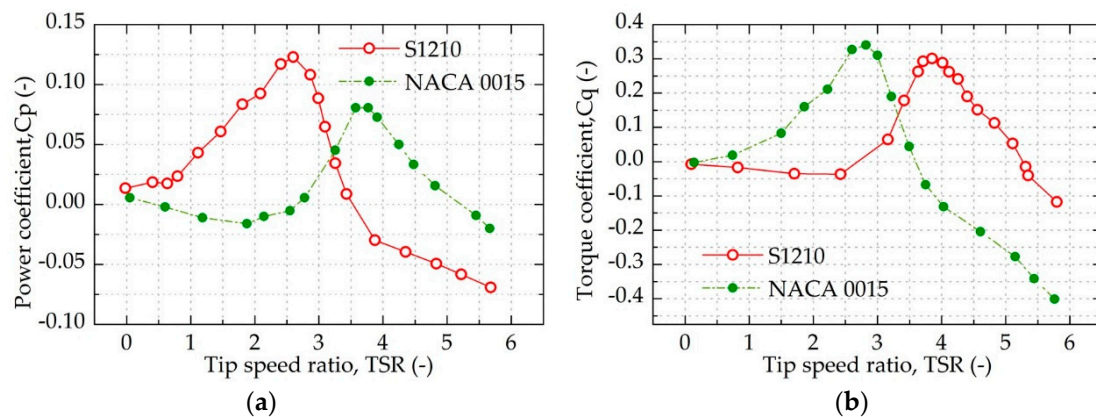


Figure 3. (a)  $C_p$  vs. TSR; (b)  $C_t$  vs. TSR for S1210 and NACA 0015 sections.

#### 4. Solidity

Solidity is defined as the ratio between the total blade area to swept area. The solidity can be achieved either by increasing the number of blades as shown in Figure 4a or increasing the chord length as displayed in Figure 4b for the given radius of the rotor. Solidity is a critical factor influencing the rotor characteristics and the immediate effect is on the tip speed ratio. Increasing the solidity of the Darrieus turbines have a negative impact on the aerodynamic performance. Ågren [32] stated that the decrease in the peak power performance is articulated to the interaction of blade with the wake generated by the preceding blade, thereby increasing the AoA and leading to the earlier stall of the following blades. Despite a notable reduction in the  $C_p$ , high solidity rotors are favored for their desirable characteristics. Mohamed [33] confirmed experimentally and numerically that increasing the number of blades generates marked increases in the static torque and high dynamic torque at low wind speeds. Increasing the solidity from  $\sigma = 0.05$  to  $\sigma = 0.2$ , the static torque coefficient ( $C_{T_s}$ ) was increased by a factor of 4, as shown in Figure 5a and the variation of power coefficient in Figure 5b, respectively. Hence to generate higher starting torque, increased number of blades are preferred. When added, a high solidity rotor is able to operate at a wider TSR, thereby extracting the energy from a larger wind speed spectrum and outputting higher annual energy. While a higher number of blades are preferred for low wind speed sites, the optimum number of blades is between two to five. The rotor rpm will be very low if the blade number is increased beyond five. As most of the Darrieus turbine is intended for electricity generation, a low rpm rotor demands a high reduction ratio gearbox or a larger permanent magnet generator if it is a direct drive power train. El-Samanoudy's [34] study on solidity reveals that increasing the number of blades from two to four led to significant power increases, but the difference between three and four blades is iota. More blades have significant aerodynamic torque loss due to the drag caused by supporting struts. While two bladed and three bladed turbines do not significantly vary in the power performance, a two-bladed turbine is not preferred from the self-starting perspective, as the self-starting capability depends on the initial starting orientation with respect to oncoming wind, as described by Worasinchai [35]. A two-bladed rotor is prone to vibrations from the unsteady loading of blades on a single plane. The cyclical peak torque for a two-bladed turbine occurs at a narrow azimuthal angle, whereas for a high solidity rotor with a higher number of blades, the torque generation happens on a wider azimuthal angle, greatly reducing the fatigue stress on the blades and support struts. Worasinchai [36] found that the optimum solidity to extract maximum energy lies between  $\sigma = 0.25$  and  $\sigma = 0.4$ . Another vital consideration is the noise, especially for the turbines intended for urban installations. Number of blades has a direct correlation on the noise generation. Mohamed [37] investigated noise from the Darrieus turbine with solidity  $\sigma = 0.1$  and  $\sigma = 0.25$  and revealed that the turbine with the solidity of  $\sigma = 0.25$  generate 7.6 dB more than  $\sigma = 0.1$  solidity turbine. The higher noise was attributed to the blade and wake interaction. A two-bladed turbine operating at a higher TSR can generate attention grabbing swishing noise. Increasing the number of blades invariably

increases the cost due to additional weight without significant increase in power, yet from the rotor dynamics and longevity of the structure, a more aesthetically pleasing three bladed rotors is an opt choice. Hence it can be concluded that for low solidity rotors, either two or three bladed can be optimum for maximizing the performance, while for low wind speed operation, high solidity rotors of four or higher number blades are preferred.

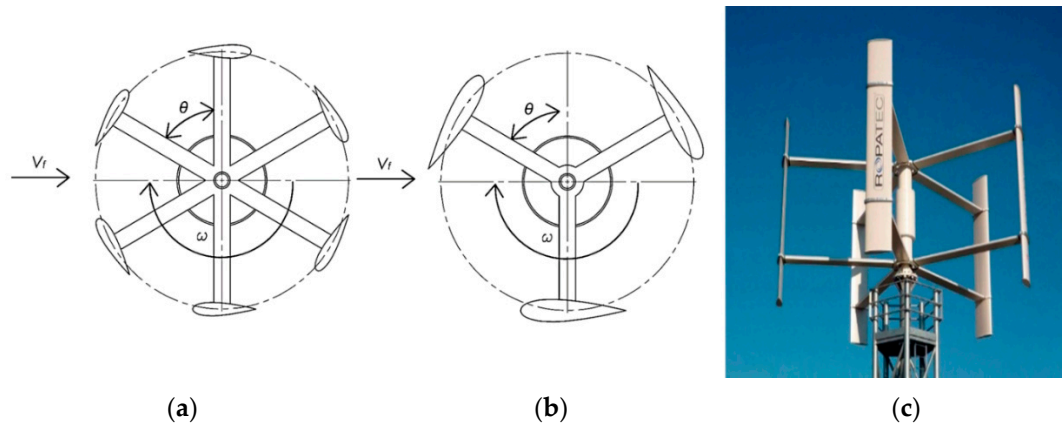


Figure 4. (a) Increased number of blades; (b) Increased chord; (c) High solidity turbine.

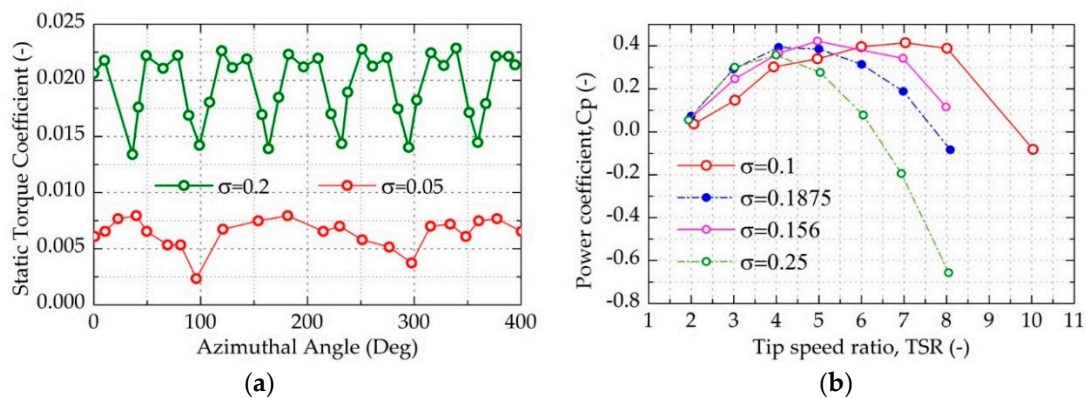


Figure 5. (a) Effect of solidity on  $C_{Ts}$ ; (b) Effect of solidity on  $C_p$ .

### 5. Helical Blades

The helical turbine was proposed by Gorlov [38] to generate starting torque, irrespective of the initial orientation of the rotor. The helical Darrieus turbine is constructed by constantly twisting the straight blades around the rotor axis as shown in Figure 6a–c. The number of blades, size of the turbine, and the airfoil characteristics dictate the swept angle. The starting torque generated is constant over 360° azimuthal positions reducing the torque ripple during continuous operation. The poor self-starting capability of a Darrieus rotor is due to the lack of total energy (E) generated by the blades to overcome the resistive torque to accelerate beyond the dead band. Baker [39] calculated the total energy that can be obtained for the Darrieus rotor, as shown in the Equation (1) with respect to the azimuthal position.

$$E = \int r q C_t(\alpha) d\theta \tag{1}$$

To increase the energy yield either the blade tangential thrust should be increased or the blade span angle  $(\alpha)d\theta$  has to be modified. The angle of inclination of the blade can be either outward or

forward as given by Equation (2) and the relative velocity ( $V$ ) as given by Equation (3).  $r$  is the radius of the turbine and  $\omega$  is the angular velocity.

$$\alpha = \sin^{-1}\left(\frac{V_f \sin \varnothing \cos \varnothing}{V}\right) \quad (2)$$

$$V = \left((r\omega - V_f \cos \varnothing)^2 + (V_f \sin \varnothing \cos \varnothing)^2\right)^{\frac{1}{2}} \quad (3)$$

The forward lean of the blades influences the airfoil characteristics as the 2D flow assumption is no longer valid due to the introduction of spanwise flow converting it into the complex 3D flow. Nevertheless, a reduction in lift coefficient was reported for such 3D flows, the stall angle is increased due to the attached boundary layer by the introduction of the spanwise flow component. For a static airfoil with the inclination of  $30^\circ$ , an increase in the stall angle from  $16^\circ$  to  $20^\circ$  was reported. Purser [40] reported that as the inclination angle was increased further, the stall angle rises to  $55^\circ$ , yielding a lift coefficient of 2.25. Shiono [41] experimentally compared the helical and straight three bladed water turbine, which shows that the straight bladed turbine has higher efficiency than the helical turbine. A maximum  $C_p$  of 0.34 can be achieved with the straight blades, whereas a helical turbine with a helix angle of  $43.7^\circ$  was able to achieve the maximum  $C_p$  of 0.16 as shown in Figure 7a. The starting characteristics comparison of the helical and the straight blade is shown in Figure 7b. Another important aspect of the helical blades is the wake pattern in the downstream and its interaction with the blades during the downstream travel. The blade wake is continuous instead of being made of vortices, as formed in the conventional straight bladed Darrieus rotor. The blade vibrations are greatly reduced due to the smooth interaction of the wake. The tangential force loading of the blade is distributed along the blade span due to a progressive shift in the AoA. The helical turbine compared to straight bladed turbines is aesthetically pleasing and well suited for the built-up environment as it is quiet in operation. On the downside [42], there are claims that the cost of manufacturing the helical blade is higher, as the manufacturing process for this blade is limited to molding, while its material is limited to composite fibers. The manufacturing cost of the blades is substantial out of the total cost of the turbine, as most small wind turbines employ a well-established aluminum extrusion process for manufacturing inexpensive blades.

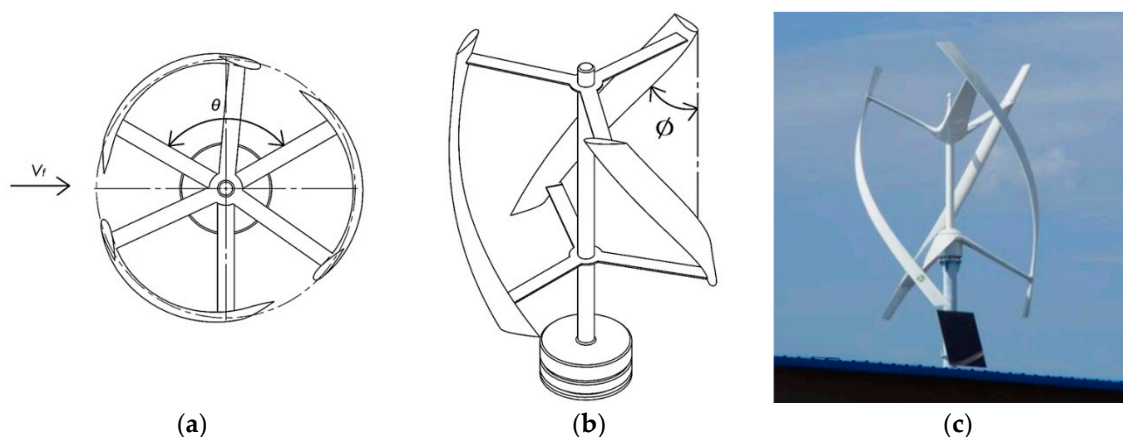


**Figure 6.** (a) Top view; (b) Front view of helical rotor; (c) Commercial helical turbine.

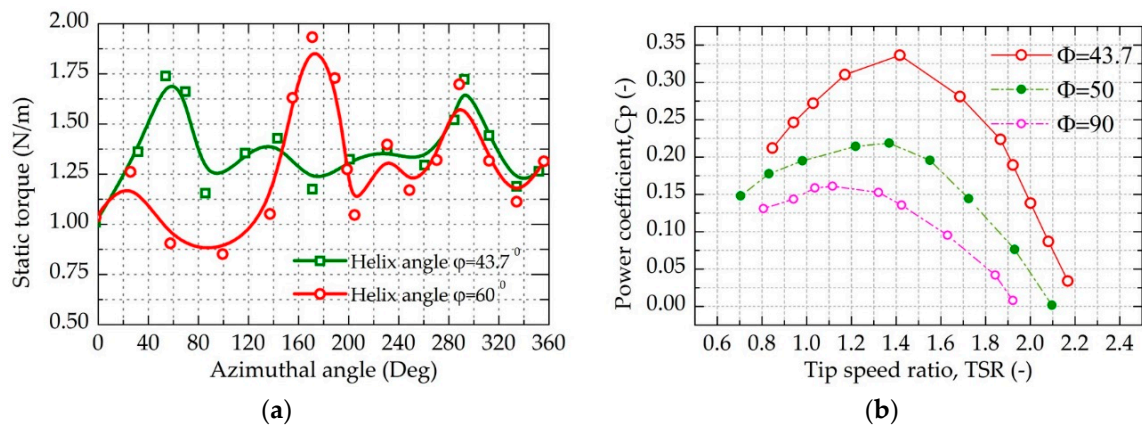
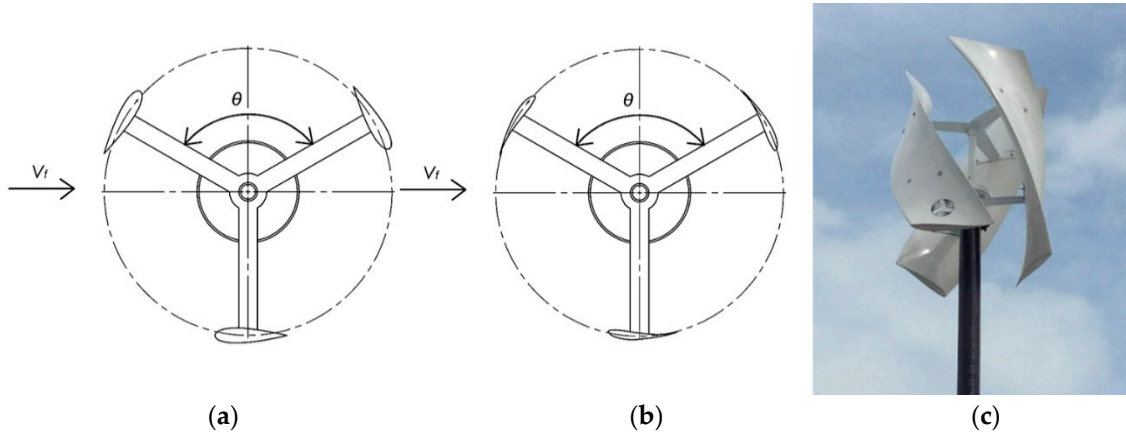


Figure 7. (a) Effect of the helical angle on starting torque (b) Effect of helical angle on  $C_p$ .

## 6. Blade Thickness

Blade thickness has a significant influence on both aerodynamic and structural characteristics. An optimum thickness should perform even in low Re for improved low wind speed operation. Top view of a Darrieus rotor with thicker and thinner airfoil is shown in Figure 8a. The airfoil thickness should be chosen cautiously, as the local relative velocity is different for the upstream and downstream halves. A thicker airfoil may perform better in the upwind half and suffer high separation bubble drag in the downwind half, especially at low TSR and high AoA. A better overall performance was displayed by 18% thick airfoil for the Re range of  $2 \times 10^5$ – $3 \times 10^5$ , as claimed by reference [31] for low wind operation. Reference [43] demonstrated that a thicker airfoil of 19% improved the starting capability than thinner airfoil. Reference [44] suggested that the maximum thickness can be increased till 28.5% without any penalty on the power coefficient and to achieve better start-up torque. The turbine loses its self-starting ability if the thickness was increased beyond this limit due to an increase in profile drag, especially at low AOA, that substantially reduces the lift/drag ratio. The effect of airfoil thickness on the starting torque was investigated by reference [45] at constant Re of  $2 \times 10^5$ . Varying thickness of symmetric NACA airfoils was tested and the results showed that thicker airfoil performs better at low Re and with an early start. As shown in Figure 9a, the thinner airfoil NACA 0012 exhibits a sudden drop in the lift coefficient, whereas the thicker airfoil such as NACA 0018 and NACA 0021 shows a smooth drop in the lift. The sudden drop will induce vibrations in the rotor, which is more pronounced when it is rotating at a relatively higher rpm. Also, it is evident from the Figure 9a that the Cl variation between NACA 0012 and NACA 0018 is minimal, but the advantages that are gained structurally are remarkable. Figure 9b shows the power coefficient comparison with TSR. The difference in the peak  $C_p$  between NACA 0012 and NACA 0018 is 16%, whereas the difference in peak  $C_p$  with NACA 0021 is 79%. The peak power coefficient is reduced as the thickness is increased but the turbine is able to operate at a wider range of TSR. There exists an optimum thickness beyond which the turbine performance decreases drastically. At a large AoA, lift-drag ratios of thinner airfoils descend sharply, while the thicker airfoils change gradually, which illustrates that the thicker airfoils perform better than the thinner ones at large AoA. In addition, for the moment curves, the larger the thickness is, the smaller the pitching moment modulus operates at with a tiny AoA, while it goes the opposite way when the AoA grows larger. Thicker airfoil also facilitates the integration of blade load alleviating devices such as actuators or flaps. As the size of the turbine grows, these devices play a critical role in reducing the blade load thereby extending blade life. A thicker airfoil will have more space to accommodate these devices. Apart from the aerodynamic gains, a thicker airfoil provides higher bending stiffness, facilitating the addition of blade spar and enhancing the overall structural characteristics. The structurally improved blades are able to withstand high centrifugal forces allowing the rotor to rotate at higher rpm. A high rpm rotor, in turn, reduces the generator and the drive train

size with significant cost savings. [46] found that the noise generated is inversely proportional to the thickness. The thicker airfoil will generate less noise compared to thinner airfoils, especially at higher TSR. Hence, an optimum airfoil thickness is 18%~20%*c* to achieve better overall performance at low wind speed and for self-starting for the small wind turbine.



**Figure 8.** (a) H-Rotor with NACA 0021 (thick) airfoil (b) H-Rotor with S1210 (thin) airfoil (c) Commercial turbine with thicker blade.

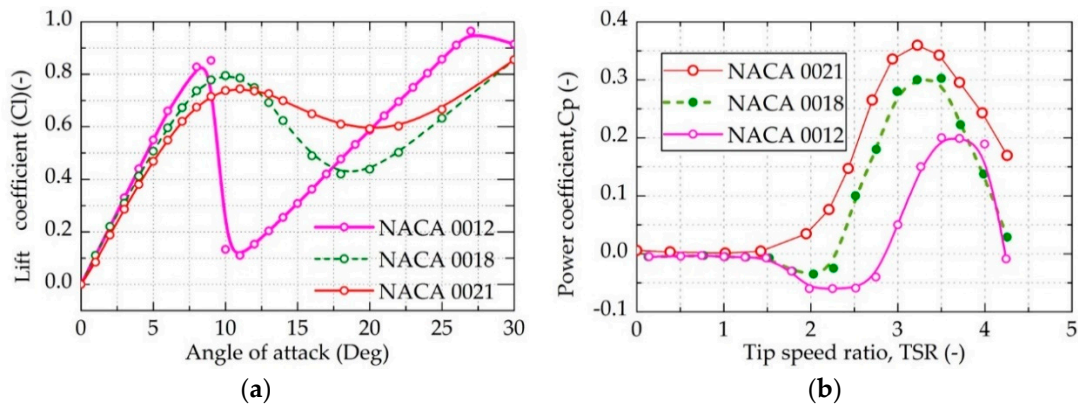


**Figure 9.** (a) Variation of  $C_l$  vs. airfoil thickness (b)  $C_p$  vs. airfoil thickness.

### 7. Vortex Generators

Vortex generators are passive devices commonly employed to delay flow separation [47]. Though airfoil stall cannot be avoided, the onset can be delayed by maximizing the energy yield of a Darrieus turbine. Apart from delaying the stall, introducing the vortex generators on the Darrieus rotor blade is of interest to increase the lift at low *Re* during the low wind speed operation and starting, as shown in Figure 9a. The principle behind any vortex generator design is to induce stream wise vortices that can exchange the high momentum fluid from free stream to relatively slower moving boundary layer. This process energizes the boundary later to overcome the adverse pressure gradient during high AoA, thus postponing the stall [48]. The dimensions of the vortex generator rely on the boundary layer thickness and may result in a drag penalty if not optimized. Though vortex generators can induce co-rotating or counter-rotating flows, the paired counter-rotating vortex generators arranged at 30° to the blade angle was most effective method, as suggested by reference [49]. An optimal chord wise position and span wise spacing are crucial in determining the performance, as shown in Figure 9b. The chord wise spacing has a greater influence on the post-stall behavior with a sudden decrease in  $C_l$  and the optimal location is found to be 30% *c* rather than 10%–15%*c*, especially at a higher AoA. The vortex generators though did not eliminate the laminar separation

bubble but it reduced the size by splitting into segments with a marked increase in the CI of 25% at  $Re\ 8 \times 10^4$ . The lift and drag characteristics of an airfoil with and without a vortex generator are shown in Figure 10a and the influence on the power generated is shown in Figure 10b. The spanwise location of the vortex generator dictates the efficiency, especially in an egg beater shaped Darrieus turbine since the root region and the equator region operates at different tip speed. A counter-rotating vortex occupying 12% blade span reported a 5% increase in annual energy output if placed at root region [50] and a 20% increase in power output at low TSR. When placed on the equator region of DAF 50 kW turbine, annual energy output fell from 7%. It is not appropriate to install VGs with the same size in different positions of blades. Though vortex generators are anticipated to improve the starting capability marginally, the peak power reduction is significant. Vortex generators are relatively simple in construction, low cost, but associated drag at higher TSR is inevitable as shown in Figure 11. Since the flow over VAWT blades is inconsistent, a detailed turbine specific numerical and experimental optimization has to be carried out to ascertain the influence on low and high TSR. The blade spoilers should not be confused with the vortex generators, as both look similar. Blade spoilers also have been investigated in DAF Indal turbine. The function of blade spoilers is to reduce the rpm of the rotor when it reaches its rated speed, and the concept was abandoned because it is not reliable to rely on aerodynamic braking. Noise has to be accounted for if it has to be installed in an urban environment. VGs incentive effect is closely related to a boundary layer thickness of the local position. VGs designed to create high turbulence will eventually increase the noise generation. A local low-pressure zone created on the blade surface will tend to demalinate the composite blades.

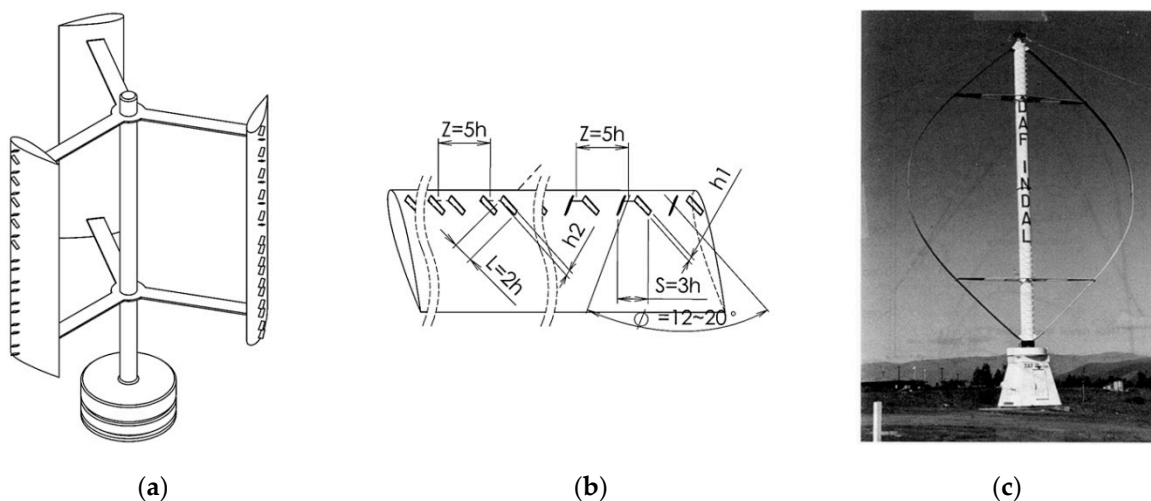


**Figure 10.** (a) H-Rotor with VG; (b) Typical VG details; (c) DAF INDAL turbine with VG.

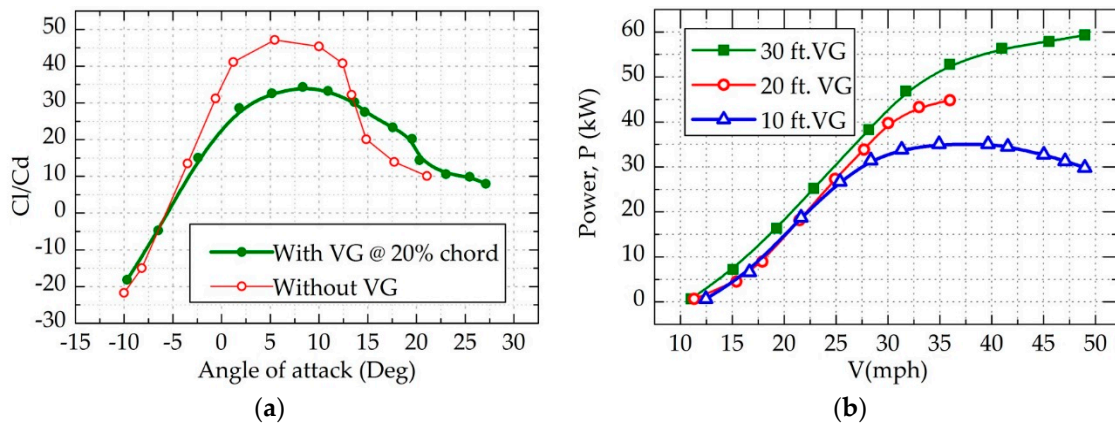


Figure 11. (a) Cl/Cd vs. AoA for with and without VG; (b) Power vs. wind speed for various VGs.

### 8. Gurney Flaps

Gurney Flaps are passive devices located at the trailing edge of an airfoil with the intention of enhancing lift as shown in Figure 12a–c. Initially employed in race car applications, these flaps are able to increase traction by altering the moment coefficient on an inverted airfoil with the high nose down pitching moment [51]. Due to its simple features in construction and operation, its applications are wide spread in subsonic, supersonic aircraft, wind turbines [52] and helicopter horizontal stabilizers. A gurney flap is a small plate mounted perpendicular to the pressure side of the airfoil at the trailing edge. The typical height of the flap will be 1–2%*c*. Though the lift coefficient continues to increase beyond 2%*c*, the associated drag increases significantly [53]. A systematic analysis of the gurney flap was performed by reference [54]. Lift augmentation is achieved by increasing the pressure on the pressure side of the airfoil and reducing the pressure on the suction side to create a recirculating counter-rotating vortex at the front and rear of the flap, especially at high AoA. Though the drag increases, the increase in lift is much higher compared to drag. It should be noted that the airfoil characteristics may differ if the airfoil encounters unsteady wind and virtual camber effects when incorporated in Darrieus turbine compared to the static airfoil. The notable positive aspect is the delay in the dynamic stall but at a maximum angle of at tack, there is a sudden drop in the lift and moment coefficient, which may lead to structural vibrations [55]. The gurney flap may generate more power, especially in the upstream stroke compared to baseline turbine without gurney flap, but may display poor performance in the downstream half. A further experimental investigation is necessary to get an insight on starting behavior and low wind speed operation with a gurney flap.

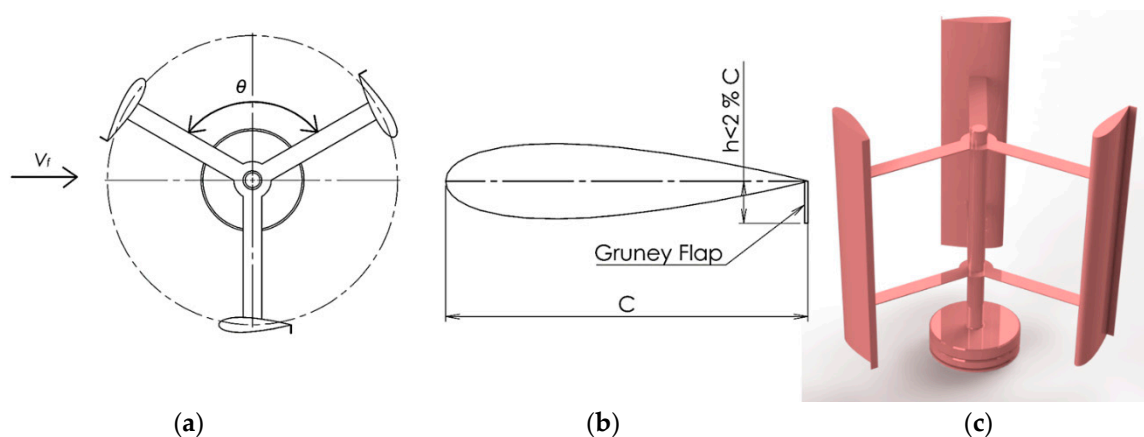


Figure 12. (a) H-rotor with Gurney flap (b) Details of an airfoil with gurney flap (c) Illustration of a H-rotor with gurney flaps.

## 9. Trailing Edge Flaps

The trailing edge flaps are active high lift devices hinged close to the trailing edge of an airfoil. The nominal length of the flap is  $10c \sim 20c$ . Initially, these flaps are employed to reduce vibrations in the helicopter rotor by varying the flap angle in relation to the flight mode [56]. The Darrieus rotor integrated with a typical trailing edge flap is shown in Figure 13a–c. Though a wide variety of flaps exists [57] a plain hinged flap is simple in construction and can be intelligently manipulated to achieve the desired airfoil characteristics. These flaps are successfully employed in HAWT for load alleviation and power control [58]. The flaps are investigated for VAWT to increase the lift at low Re and load regulation at high winds. Closed loop flaps have the potential to increase the starting torque by sensing the wind direction and altering the flap angle accordingly. Overall turbine performance can be improved by varying these flaps with respect to the azimuthal position to reduce the negative performance in the downstream half. The change in the AoA due to new chord line is given by the Equation (4).

$$\Delta\alpha = \frac{d\alpha}{d\theta} = \arctan\left(\frac{\sin\theta}{3 + \cos\theta}\right) \quad (4)$$

The nominal AoA as a function of azimuthal angle is obtained by Equation (5)

$$\alpha = \alpha_0 + \Delta\alpha = \arctan\left(\frac{\cos\Psi}{\lambda + \cos\psi}\right) + \arctan\left(\frac{\sin\theta}{3 + \cos\theta}\right) \quad (5)$$

Yang [59] conducted a 2D computational study on VAWT with trailing edge flaps and the results are encouraging. The study compared the trailing edge flap at the  $1/4c$  location from the trailing edge on NACA 0012 blade at 10 m/s with unmodified NACA 0012. The airfoil characteristics and the power coefficient variation with TSR is depicted in Figure 14a,b respectively. The average lift coefficient of NACA 0012 with a flap is increased by 0.15 and the maximum lift to drag ratio is increased by 73.

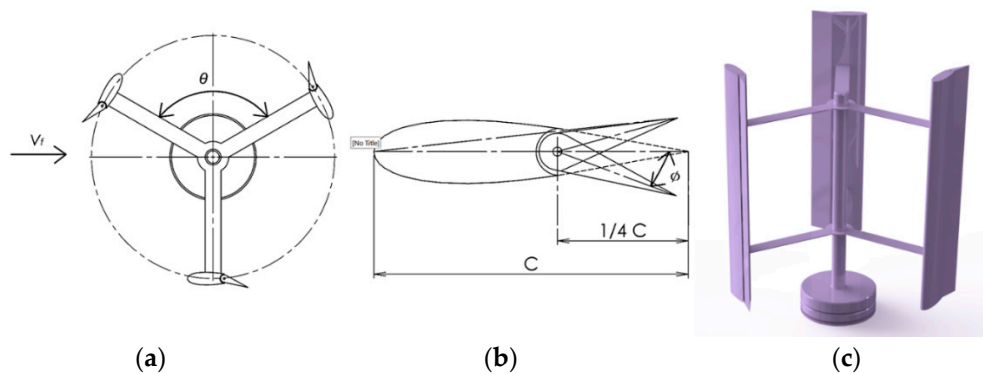


**Figure 13.** (a) H-rotor with a trailing edge flap (b) Details of an airfoil with a trailing edge flap (c) Illustration of a H-rotor with trailing edge flaps.

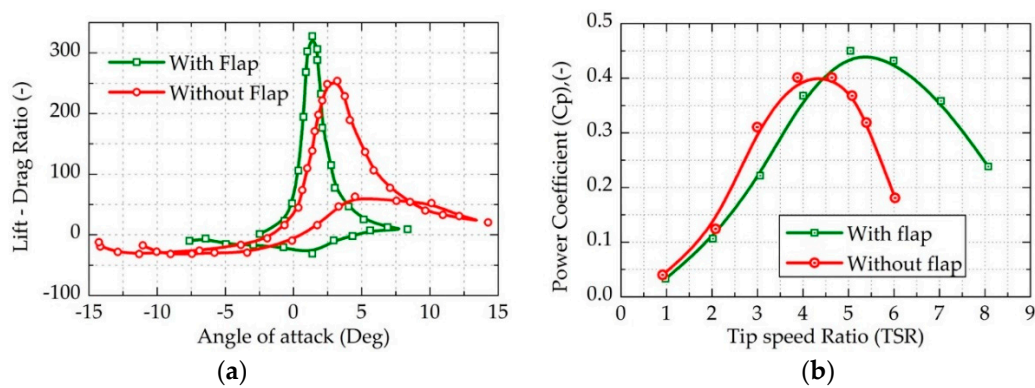


**Figure 14.** (a)  $C_l$  and  $C_d$  of NACA 0012 with and without a trailing edge flap (b)  $C_p$  vs. TSR for NACA 0012 with and without a trailing edge flap.

With the flap control, the peak power coefficient is enhanced by 10% at a higher TSR compared to the conventional blade. The power improvement is attributed to the delay in the dynamic stall and by the minimization of blade vortex interaction. The implementation of trailing edge flaps to straight bladed turbine is dictated by the size of the turbine. The trailing edge flaps are not possible to integrate into the helical blades as the hinge axis of the flap is twisted along the rotor axis and it is highly complicated due to actuation and blade loading. Though it is widely employed in HAWT, the flaps are mostly installed on the portion on the blade with minimum twist, which is mostly at the tip of the blade, where the twist variation is minimal compared to the blade span. The use of trailing edge flaps along with individual blade pitching on HAWT is expected to find its place, especially for the turbines of 8 MW. The initial computational study sheds the light on the applicability of trailing edge flaps for Darrieus turbine and a possible means of achieving overall turbine performance at low wind speed assuring a good start for further study. Dynamically varying trailing edge flaps have to be studied in detail, influencing the whole sections of the blade.

## 10. J-Blade

The J profiled blades are formed by removing a portion of the blade from the trailing edge either on the pressure side or suction side of the conventional airfoil. The objective of introducing such an opening is to increase the starting torque and power generation at low wind speed in the range of 3–5 m/s, especially for small wind turbines. The opening can be continuous for the entire blade span or intermittent dictated by the blade thickness, startup wind speed and structural requirements. Figure 15a,c displays an H-Darrieus with incorporated J profiled blade. The J-blades operates both in lift and drag mode and exhibits a lower lift/drag ratio compared to its parent conventional airfoil due to a reduced lift and higher form drag. Zamani [60] performed a computational study on DU-06-W-200 airfoil and the J-profile airfoil J-DU-06-W-200 derived from it. The drag coefficient for J-DU-06-W-200 is lower than DU-06-W-200 when compared for a 3 kW turbine at  $Re\ 5 \times 10^5$ . The results indicate that the torque amplitude is widened for larger azimuthal angles reducing the vibration and fatigue stress in the case of J-DU-06-W-200 but the operating TSR range as is reduced from 4 to 3.5, as indicated in Figure 16a. The performance of the turbine is greatly influenced by the location of the opening and the blade thickness. A thicker blade has a wider drag bucket and tends to generate higher static torque. The study on NACA0015 by Zamani [61] with 250 mm chord concluded wake region on the rear of the rotor decreases due to vortices trapped in the opening. Chen [62] studied the opening ration and suggested that for the turbines operating at higher TSR and from the self-starting perspective, an inner opening ratio which is defined by the ratio of opening length ( $h$ ) to the distance from the leading edge ( $s$ ) should be 0.48 to 0.60. For the turbines operating at low TSR and dominated by drag with the objective of replacing the Savonius turbine, an outer opening ratio of 0.72 to 0.84 is optimal. Though larger opening will generate higher torque, trade-off should be made with the  $C_p$

loss. An added advantage is from the inexpensive manufacturing process. Since the opening facilitates easy access, the blades can be manufactured by bending aluminum sheet over a precut profile that performs the function of ribs to strengthen the blade. This manufacturing process can significantly curtail the manufacturing cost compared to traditional glass fiber moulding process. The J-Blade was implemented commercially and has been proven to be efficient, especially for small wind turbines, compared to the Hybrid Darrieus-Savonius turbine. Application of J-Blades for higher kW capacity turbines requires further optimization study at high Re and TSR. Based on the above findings, it appears that the desirable rotors for inner opening are the rotors with 0.48 and 0.60 inner opening ratios. The rotors with 0.72 and 0.84 outer opening ratios seem to be the promising devices and can be used to replace the Savonius- Darrieus rotor considering the  $C_p$  loss and the increase of the  $C_{T_s}$ . The strategies briefed so far have been compared in the Table 1.

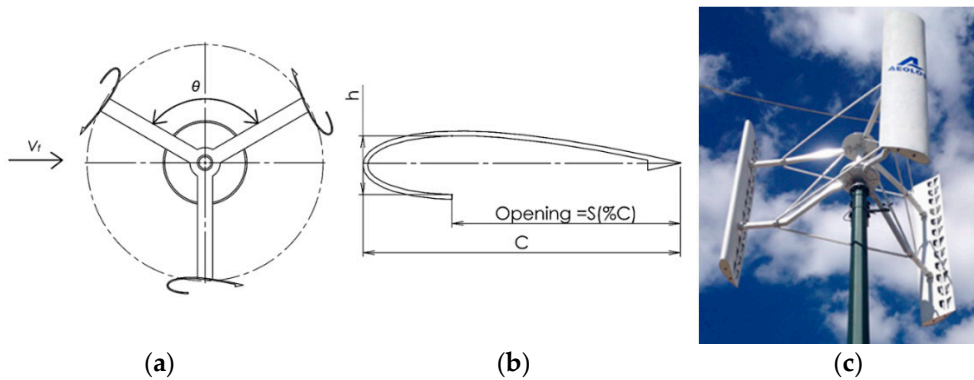


Figure 15. (a) H-Rotor with J-profile airfoil (b) Details of J-profile airfoil (c) Commercial turbine with J-profiled blade.

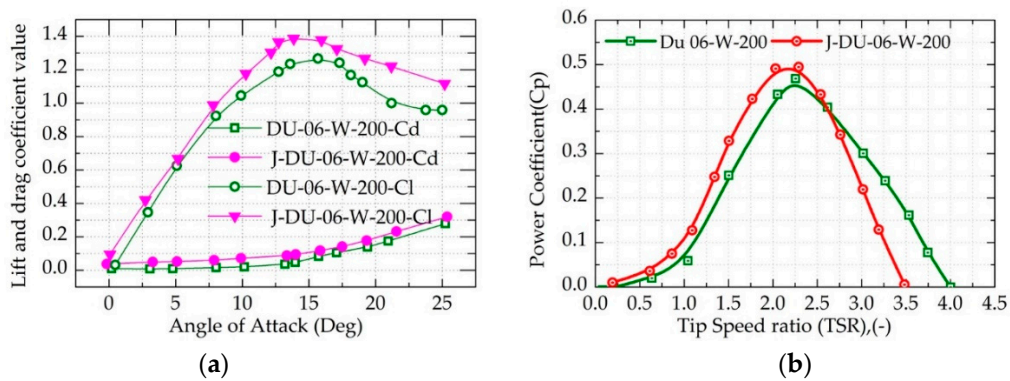


Figure 16. (a)  $C_l$  and  $C_d$  of J-profile blade, (b)  $C_p$  vs. TSR comparison with parent airfoil.

**Table 1.** Comparison of strategies, their merits, and demerits.

Strategy	Merits	Demerits
Airfoil characteristics	Less complex, cost-effective, better optimization of dynamic stall, blade tip loss. Increased structural rigidity	Minimal improvement in starting performance and overall power coefficient
Cambered airfoil	Better starting capability delayed stall, less sensitive to surface roughness, high pitching moment	Increased drag on the down half, reduction in power coefficient
Solidity	Increased starting torque, low centrifugal forces due to low rpm	Large AoA, large drive train size and additional cost due to an increased number of blades
Helical blades	Improved aesthetics, smooth torque pulsation leading to reduced vibration	High manufacturing cost of blades, low torque for every azimuthal position
Blade thickness	Better performance at low Re delayed stall and structurally sound	Increased profile drag at high Re and noise
Vortex generators	Improved performance at low Re, extended dynamic stall and marginal improvement in starting torque	Increased drag at high TSR and increases noise due to vortex shedding
Gurney flaps	Delayed dynamic stall with an increase in starting torque compared to a conventional airfoil	Vibration after stall and noise due to vortex shedding
Trailing edge flaps	Better performance in high and low TSR, able to regulate the rotor rpm aerodynamically	Power has to be expended to operate flaps, requires a sophisticated control system
J-Blade	Excellent startup torque, able to sustain low wind speed rotation, ease of blade manufacturing	Degraded performance at high TSR due to high form drag at high Re and increased fatigue failure of blades

## 11. Conclusions

The Darrieus wind turbine has experienced ups and downs since its invention. Several critical issues hindering the development of H-Darrieus have been addressed in the past years. During the 1980s when the research on Darrieus turbine was at a peak, blade failures were a recurrent problem due to cyclic stress, which almost brought the research on these turbines to a halt. This happened because aluminum is the predominant blade material, which is not able to withstand the alternating stress, leading to premature failure. Due to advancements in the composites and the invention of glass and carbon fiber composites, a solution remedying blade was found. The next immediate challenge is to enhance the poor performance of these turbines at low wind speeds and its starting characteristics, which is still a challenge to the research community. The starting of VAWTs is described as a transition process from linear flow, at low TSR, to rotational flow, at high TSR, which involves the change of a vertical structure of wake and blade–wake interaction. The current review discusses the proposed solutions and its drawbacks for an early start in detail. The emphasis in this review is placed on the starting torque comparison and its influence on the power coefficient. A large number of papers have been published in several key areas such as aerodynamics, control systems, and generator design with a strong focus on the development of Darrieus turbine for low wind speeds. The innovative concepts discussed in the current text will provide the readers with adequate knowledge on choosing the suitable mechanisms to enhance the performance at weak winds. Since only a handful of concepts have been discussed in this current text, the study is intended to cover almost all the concepts by extending it to part 2 and part 3. H-Darrieus with enhanced low wind performance has much better prospects than HAWT.

**Author Contributions:** Funding acquisition, S.R. and W.H.; Project administration, W.H.; Supervision, L.T.-C.; Writing—original draft, M.P.; Writing—review & editing, K.S.

**Funding:** This research was funded by 2016 ASTAR AME IRG Grant- A1783c0012.

**Conflicts of Interest:** The authors declare no conflict of interest.

## References

- Li, Y.; Wu, X.-P.; Li, Q.-S.; Tee, K.F. Assessment of onshore wind energy potential under different geographical climate conditions in China. *Energy* **2018**, *152*, 498–511. [[CrossRef](#)]
- Noyes, C.; Qin, C.; Loth, E. Pre-aligned downwind rotor for a 13.2 MW wind turbine. *Renew. Energy* **2018**, *116*, 749–754. [[CrossRef](#)]
- Korprasertsak, N.; Leephakpreeda, T. Analysis and optimal design of wind boosters for Vertical Axis Wind Turbines at low wind speed. *J. Wind Eng. Ind. Aerodyn.* **2016**, *159*, 9–18. [[CrossRef](#)]
- Mohan Kumar, P.; Surya, M.M.R.; Narasimalu, S.; Lim, T.-C. Experimental and numerical investigation of novel Savonius wind turbine. *Wind Eng.* **2018**, *43*, 247–262. [[CrossRef](#)]
- Kumar, P.M.; Purimitla, S.R.; Shubhra, S.; Srikanth, N. Numerical and analytical study on telescopic savonius turbine blade. In Proceedings of the 2017 3rd International Conference on Power Generation Systems and Renewable Energy Technologies (PGSRET), Johor Bahru, Malaysia, 4–6 April 2017; pp. 107–112.
- Joo, S.; Choi, H.; Lee, J. Aerodynamic characteristics of two-bladed H-Darrieus at various solidities and rotating speeds. *Energy* **2015**, *90*, 439–451. [[CrossRef](#)]
- Kumar, P.M.; Sivalingam, K.; Narasimalu, S.; Lim, T.C.; Ramakrishna, S.; Wei, H. A Review on the Evolution of Darrieus Vertical Axis Wind Turbine: Small Wind Turbines. *J. Power Energy Eng.* **2019**, *7*, 27–44. [[CrossRef](#)]
- Islam, M.; Ting, D.S.; Fartaj, A. Desirable airfoil features for smaller-capacity straight-bladed VAWT. *Wind Eng.* **2007**, *31*, 165–196. [[CrossRef](#)]
- Laneville, A.; Vittecoq, P. Dynamic stall: The case of the vertical axis wind turbine. *J. Sol. Energy Eng.* **1986**, *108*, 140–145. [[CrossRef](#)]
- Timmer, W.; Van Rooij, R. Summary of the Delft University wind turbine dedicated airfoils. *ASME-J. Sol. Energy Eng.* **2003**, *125*, 488–496. [[CrossRef](#)]
- Jasinski, W.J.; Noe, S.C.; Selig, M.S.; Bragg, M.B. Wind turbine performance under icing conditions. *Trans.-ASME-J. Sol. Energy Eng.* **1998**, *120*, 60–65. [[CrossRef](#)]
- Shepherd, D.; McBride, D.; Welch, D.; Dirks, K.N.; Hill, E.M. Evaluating the impact of wind turbine noise on health-related quality of life. *Noise Health* **2011**, *13*, 333. [[CrossRef](#)] [[PubMed](#)]
- Kato, Y.; Seki, K. Vertical axis wind turbine designed aerodynamically at Tokai University. *Period. Polytech. Mech. Engi.* **1981**, *25*, 47–56.
- Snyder, M.H.; Furukawa, N. *WER-6: Comparison of Performance of Darrieus Wind Turbines Having 12% and 21% Thick Sections*; Center for Energy Studies, Wichita State University: Wichita, Kansas, 1979.
- Sheldahl, R.E.; Klimas, P.C. *Aerodynamic Characteristics of Seven Symmetrical Airfoil Sections through 180-Degree Angle of Attack for Use in Aerodynamic Analysis of Vertical Axis Wind Turbines*; Sandia National Labs.: Albuquerque, NM, USA, 1981.
- Sutherland, H.J.; Berg, D.E.; Ashwill, T.D. *A Retrospective of VAWT Technology*; Sandia Report No. SAND2012-0304; Sandia National Laboratories: Albuquerque, NM, USA, 2012.
- Kumar, P.M.; Rashmitha, S.R.; Srikanth, N.; Lim, T.-C. Wind Tunnel Validation of Double Multiple Streamtube Model for Vertical Axis Wind Turbine. *Smart Grid Renew. Energy* **2017**, *8*, 412. [[CrossRef](#)]
- Migliore, P. Comparison of NACA 6-series and 4-digit airfoils for Darrieus wind turbines. *J. Energy* **1983**, *7*, 291–292. [[CrossRef](#)]
- Zervos, A. Aerodynamic evaluation of blade profiles for vertical axis wind turbines. In Proceedings of the European Community Wind Energy Conference, Herning, Denmark, 6–10 June 1988; pp. 611–616.
- Claessens, M. The Design and Testing of Airfoils for Application in Small Vertical Axis Wind Turbines. Master's Thesis, Delft University of Technology, Delft, The Netherlands, 2006.
- McGhee, R.J.; Beasley, W.D. *Wind-Tunnel Results for a Modified 17-Percent-Thick Low-Speed Airfoil Section*; NASA Langley Research Center: Hampton, VA, USA, 1981.
- Singh, M.; Biswas, A.; Misra, R. Investigation of self-starting and high rotor solidity on the performance of a three S1210 blade H-type Darrieus rotor. *Renew. Energy* **2015**, *76*, 381–387. [[CrossRef](#)]
- Kumar, M.; Surya, M.M.R.; Sin, N.P.; Srikanth, N. Design and experimental investigation of airfoil for extruded blades. *Int. J. Adv. Agric. Environ. Eng. (IJAAEE)* **2017**, *3*, 2349–2523.
- Kumar, P.M.; Surya, M.M.R.; Srikanth, N. On the improvement of starting torque of darrieus wind turbine with trapped vortex airfoil. In Proceedings of the 2017 IEEE International Conference on Smart Grid and Smart Cities (ICSGSC), Singapore, 23–26 July 2017; pp. 120–125.

25. Kumar, P.M.; Surya, M.M.R.; Kethala, R.; Srikanth, N. Experimental investigation of the performance of darrieus wind turbine with trapped vortex airfoil. In Proceedings of the 2017 3rd International Conference on Power Generation Systems and Renewable Energy Technologies (PGSRET), Johor Bahru, Malaysia, 4–6 April 2017; pp. 130–135.
26. Kumar, P.M.; Kulkarni, R.; Srikanth, N.; Lim, T.-C. Performance Assessment of Darrieus Turbine with Modified Trailing Edge Airfoil for Low Wind Speeds. *Smart Grid Renew. Energy* **2017**, *8*, 425. [[CrossRef](#)]
27. Kumar, P.M.; Surya, M.M.R.; Srikanth, N. Comparitive CFD analysis of darrieus wind turbine with NTU-20-V and NACA0018 airfoils. In Proceedings of the 2017 IEEE International Conference on Smart Grid and Smart Cities (ICSGSC), Singapore, 23–26 July 2017; pp. 108–114.
28. Rainbird, J.M.; Bianchini, A.; Balduzzi, F.; Peiró, J.; Graham, J.M.R.; Ferrara, G.; Ferrari, L. On the influence of virtual camber effect on airfoil polars for use in simulations of Darrieus wind turbines. *Energy Convers. Manag.* **2015**, *106*, 373–384. [[CrossRef](#)]
29. Islam, M.; Ting, D.S.; Fartaj, A. Design of a special-purpose airfoil for smaller-capacity straight-bladed VAWT. *Wind Eng.* **2007**, *31*, 401–424. [[CrossRef](#)]
30. Kirke, B.K. *Evaluation of Self-Starting Vertical Axis Wind Turbines for Stand-Alone Applications*; Griffith University Australia: Queensland, Australia, 1998.
31. Healy, J. The influence of blade camber on the output of vertical-axis wind turbines. *Wind Eng.* **1978**, *2*, 146–155.
32. Ågren, O.; Berg, M.; Leijon, M. A time-dependent potential flow theory for the aerodynamics of vertical axis wind turbines. *J. Appl. Phys.* **2005**, *97*, 104913. [[CrossRef](#)]
33. Mohamed, M. Impacts of solidity and hybrid system in small wind turbines performance. *Energy* **2013**, *57*, 495–504. [[CrossRef](#)]
34. El-Samanoudy, M.; Ghorab, A.; Youssef, S.Z. Effect of some design parameters on the performance of a Giromill vertical axis wind turbine. *Ain Shams Eng. J.* **2010**, *1*, 85–95. [[CrossRef](#)]
35. Worasinchai, S.; Ingram, G.L.; Dominy, R.G. The Physics of H-Darrieus Turbine Starting Behavior. *J. Eng. Gas Turbines Power* **2015**, *138*, 062605. [[CrossRef](#)]
36. Staelens, Y.; Saeed, F.; Paraschivoiu, I. A Straight-Bladed Variable-Pitch VAWT Concept for Improved Power Generation. *AIAA Pap.* **2003**, 146–154. [[CrossRef](#)]
37. Mohamed, M. Aero-acoustics noise evaluation of H-rotor Darrieus wind turbines. *Energy* **2014**, *65*, 596–604. [[CrossRef](#)]
38. Gorlov, A. *Development of the Helical Reaction Hydraulic Turbine. Final Technical Report, 1 July 1996–30 June 1998*; Northeastern University: Boston, MA, USA, 1998.
39. Baker, J. Features to aid or enable self starting of fixed pitch low solidity vertical axis wind turbines. *J. Wind Eng. Ind. Aerodyn.* **1983**, *15*, 369–380. [[CrossRef](#)]
40. Purser, P.E.; Spearman, M.L. *Wind-Tunnel Tests at Low Speed of Swept and Yawed Wings Having Various Plan Forms*; NASA: Washington, DC, USA, 1951.
41. Shiono, M.; Suzuki, K.; Kiho, S. Output characteristics of Darrieus water turbine with helical blades for tidal current generations. In Proceedings of the Twelfth International Offshore and Polar Engineering Conference, Kitakyushu, Japan, 26–31 May 2002.
42. Blackwell, B.; Reis, G. *Blade Shape for a Troposkien Type of Vertical-Axis Wind Turbine*; Sandia Labs.: Albuquerque, NM, USA, 1974.
43. Danao, L.A.; Qin, N.; Howell, R. A numerical study of blade thickness and camber effects on vertical axis wind turbines. *Proc. Inst. Mech. Eng. Part A J. Power Energy* **2012**, *226*, 867–881. [[CrossRef](#)]
44. Batista, N.; Melício, R.; Marias, J.; Catalão, J. Self-start evaluation in lift-type vertical axis wind turbines: Methodology and computational tool applied to asymmetrical airfoils. In Proceedings of the Power Engineering, Energy and Electrical Drives (POWERENG), 2011 International Conference, Malaga, Spain, 11–13 May 2011; pp. 1–6.
45. Alam, M.; Iqbal, M. A low cut-in speed marine current turbine. *J. Ocean Technol.* **2010**, *5*, 49–61.
46. Parchen, R.; Bruggeman, J.; Dassen, A. The effect of the blade thickness of wind turbine blades on the noise due to inflow turbulence. *Acustica* **1996**, *82*, S82.
47. Mueller-Vahl, H.; Pechlivanoglou, G.; Nayeri, C.; Paschereit, C. *Vortex Generators for Wind Turbine Blades: A Combined Wind Tunnel and Wind Turbine Parametric Study*; ASME Paper No. GT2012-69197; American Society of Mechanical Engineers: New York, NY, USA, 2012.

48. Quinlan, P.; Scheffler, R.; Wehrey, M. Performance Test Results of Vortex Generators Attached to a Vertical Axis Wind Turbine. In Proceedings of the 7th ASME Wind Energy Symposium, New Orleans, LA, USA, 10–13 January 1988; p. 16.
49. Seshagiri, A.; Cooper, E.; Traub, L.W. Effects of vortex generators on an airfoil at low Reynolds numbers. *J. Aircr.* **2009**, *46*, 116. [[CrossRef](#)]
50. Paraschivoiu, I. *Wind Turbine Design: With Emphasis on Darrieus Concept*; International Polytechnic Press: Quebec, Canada, 2002.
51. Zerihan, J.; Zhang, X. Aerodynamics of Gurney flaps on a wing in ground effect. *AIAA J.* **2001**, *39*, 772–780. [[CrossRef](#)]
52. Zayas, J.; Van Dam, C.; Chow, R.; Baker, J.; Mayda, E. Active aerodynamic load control for wind turbine blades. In Proceedings of the European Wind Energy Conference, Athens, Greece, 27 February–2 March 2006.
53. Liu, T.; Montefort, J. Thin-airfoil theoretical interpretation for Gurney flap lift enhancement. *J. Aircr.* **2007**, *44*, 667–671. [[CrossRef](#)]
54. Liebeck, R.H. Design of subsonic airfoils for high lift. *J. Aircr.* **1978**, *15*, 547–561. [[CrossRef](#)]
55. Xu, Z.; Wang, Q.; Dai, G.; Tan, H.; Zhong, Y. Study on improvement in aerodynamic performance of Vertical Axis Wind Turbine using Gurney flap. In Proceedings of the 2011 Second International Conference on Mechanic Automation and Control Engineering, Hohhot, China, 15–17 July 2011; pp. 6884–6887. [[CrossRef](#)]
56. Viswamurthy, S.R.; Ganguli, R. An optimization approach to vibration reduction in helicopter rotors with multiple active trailing edge flaps. *Aerosp. Sci. Technol.* **2004**, *8*, 185–194. [[CrossRef](#)]
57. Joncas, S.; Bergsma, O.; Beukers, A. Power regulation and optimization of offshore wind turbines through trailing edge flap control. In Proceedings of the 43th AIAA Aerospace Science Meeting and Exhibit, Reno, NV, USA, 10–13 January 2005; pp. 10–13.
58. Castaignet, D.; Barlas, T.; Buhl, T.; Poulsen, N.K.; Wedel-Heinen, J.J.; Olesen, N.A.; Bak, C.; Kim, T. Full-scale test of trailing edge flaps on a Vestas V27 wind turbine: Active load reduction and system identification. *Wind Energy* **2014**, *17*, 549–564. [[CrossRef](#)]
59. Yang, Y.; Li, C.; Zhang, W.; Guo, X.; Yuan, Q. Investigation on aerodynamics and active flow control of a vertical axis wind turbine with flapped airfoil. *J. Mech. Sci. Technol.* **2017**, *31*, 1645–1655. [[CrossRef](#)]
60. Zamani, M.; Maghrebi, M.J.; Varedi, S.R. Starting torque improvement using J-shaped straight-bladed Darrieus vertical axis wind turbine by means of numerical simulation. *Renew. Energy* **2016**, *95*, 109–126. [[CrossRef](#)]
61. Zamani, M.; Nazari, S.; Moshizi, S.A.; Maghrebi, M.J. Three dimensional simulation of J-shaped Darrieus vertical axis wind turbine. *Energy* **2016**, *116*, 1243–1255. [[CrossRef](#)]
62. Chen, J.; Yang, H.; Yang, M.; Xu, H. The effect of the opening ratio and location on the performance of a novel vertical axis Darrieus turbine. *Energy* **2015**, *89*, 819–834. [[CrossRef](#)]

